Journal of Quality Engineering and Production Optimization

Volume 8, Issue 2, Summer & Autumn 2023

http://jqepo.shahed.ac.ir

Research Paper

DOI: 10.22070/jqepo.2024.18982.1277

A new composite index for improved capability analysis of profile coefficients

Aylin Pakzad [1]

[1] *Department of Industrial Engineering, Kosar University of Bojnord, Bojnord, Iran*

**** Corresponding Author:*** *Aylin Pakzad (Email: a.pakzad@kub.ac.ir)*

Abstract *–A simple linear profile (SLP) is a type of quality profile that describes the relationship between a response variable and an explanatory variable using a linear function. This concept is relevant in various industrial applications. Process capability indices (PCIs) are useful tools for measuring the process ability in producing items in conformance within the pre-set specification limits (SLs). In this paper, a composite PCI is presented for a SLP based on its parameters. The performance of the proposed PCI and existing ones are investigated and compared for their accuracy and precision of estimation. The simulation results highlight the superior performance of the proposed composite PCI to existing methods in terms of lower mean absolute error (MAE) and mean square error (MSE) metrics. Two real-world case studies are also analyzed to demonstrate how the proposed method can be applied in practice.*

Keywords*– Composite capability index, Simple linear profile (SLP), Specification limits (SLs), Simulation studies.*

I. INTRODUCTION

In many practical applications, quality characteristics of interest are usually described by a relationship between a response variable(s) and one or more explanatory variables referred to as "profile". There are various types of profiles, including simple linear profiles (SLPs), polynomial profiles, multiple profiles, and nonlinear profiles. This study focuses on SLPs, which can be modeled using a simple linear regression. In this model, a single explanatory variable X is used to describe the behavior of the response variable Y (Saghaei and Noorossana, 2011). Generally, profile monitoring involves two phases (Woodall et al., 2004). In Phase I, the stability of the process is assessed, and the unknown profile parameters are estimated. Subsequently, in Phase II, the focus shifts to detecting potential shifts in the in-control process parameters as they occur (Saghaei and Noorossana, 2011).

Profile monitoring has been extensively studied by many researchers, and several methods have been developed for monitoring different profiles in both phases I and II (Abbasi et al., 2021; Derakhshani et al., 2021; Fakhimikazemi et al., 2023; Sogandi and Amiri, 2023; Yeganeh et al., 2024; Yeganeh and Shadman, 2021). For a more in-depth understanding of profile monitoring, readers are encouraged to consult the literature review by (Maleki et al., 2018).

Manuscript Received:17-August-2023 & Revised: 9-October-2023 & Accepted: 20-December-2023
ISSN: 2423-3781

Process capability analysis (PCA) is a critical aspect of statistical process control, used to evaluate a process's ability to consistently produce products within specification limitations (SLs). Process capability indices (PCIs) are numerical measures generated through PCA to assess process performance relative to these tolerances. Higher PCI values indicate better process capability. Research on PCIs has encompassed both single and multiple quality characteristics, as well as complex product attributes known as profiles. Previous studies, such as (De-Felipe and Benedito, 2017; Pakzad et al., 2021) have provided comprehensive overviews of PCI development for these various product types.

Assessment of process capability for in-control SLP was started by Shahriari and Sarrafian (2009). Following that, Ebadi and Shahriari (2013) proposed two methods for assessing the capability of SLPs, based on the observed response and the predicted response variable. Hosseinifard and Abbasi (2012a) estimated PCI for SLP using the proportion of nonconformance in another attempt. Furthermore, five approaches to estimating PCIs for non-normal linear profiles were examined and contrasted by Hosseinifard and Abbasi (2012b).

Process yield, or the proportion of conforming products, is a standard metric for evaluating manufacturing process capability. Assuming a normal distribution, process yield can be calculated by $\%\text{Yield} = \Phi((USL - \mu)/\sigma) - \Phi((\mu - LSL)/\sigma)$, where USL and LSL are the upper and lower SLs, respectively, μ is the process mean, σ is the process standard deviation, and $\Phi(.)$ is the cumulative distribution function (CDF) of the standard normal distribution. Previous research has extended the concept of process yield to linear profiles, considering both simple and multivariate cases, as well as accounting for autocorrelation within and between profiles (Wang, 2014, 2016; Wang and Tamirat, 2014, 2015). Ganji and Gildeh (2023) introduced a new competence index for SLPs, which outperforms the indices proposed by Ebadi and Shahriari (2013) and Wang (2014) in terms of precision and accuracy.

A functional approach was initially introduced by Nemati Keshteli et al. (2014) to evaluate the capability of linear profile processes by considering the entire range of the explanatory variable. This method has been extended to assess other profile types, including circular and nonlinear profiles (Nemati Keshteli et al. 2014b; Pour Larimi et al. 2019; Wang, 2015). Subsequent research focused on developing functional loss-based capability indices for linear profiles with symmetric and asymmetric tolerances, incorporating bootstrap confidence intervals to enhance reliability (Pakzad and Basiri, 2023; Pakzad et al., 2022).

Recently, many studies are developed PCIs for other types of profiles, including logistic regression profiles (Amiri and Rezaye Abbasi Charkhi, 2015; Rezaye Abbasi Charkhi et al., 2016), Poisson regression profiles (Alevizakos et al., 2019), nonlinear profile (Guevara G and Alejandra López, 2022; Guevara and Vargas, 2016; Guevara and Vargas, 2015; Wang and Guo, 2014), and SLP in multi-stage processes (Adibfar and Noorossana, 2022, 2024).

Previous research (Chiang et al., 2017; Karimi Ghartemani et al., 2016; Wu, 2016) has treated process capability analysis for SLPs as a problem involving two correlated variables: the intercept and slope. This approach has led to the development of PCIs for SLPs based on multivariate PCI methods. However, these previous studies have been criticized for not accurately determining the SLs for the profile parameters.

Recent work has addressed this issue by considering both profile SLs and in-control profile information to establish more accurate SLs for the intercept and slope. This led to the proposal of two univariate indices $C_{pm_{b_0}}$ and $C_{pm_{b_1}}$ for evaluating SLP capability based on the intercept and slope separately. A process is deemed incapable if either index falls below a certain threshold.

This paper introduces a method to produce one number jointly representing SLP capability based on its parameters, which also improves the estimators of PCIs. To this end, a new composite index for the SLP intercept and slope parameters is established. While acknowledging the potential for bias, the proposed index aims to enhance the accuracy of process capability estimation by reducing mean squared error (MSE) compared to existing methods. The proposed method combines the strengths of Bothe's multivariate PCI (Bothe, 1999) with the accurate SL estimation from (Pakzad et al., 2024) to provide an improved single index for assessing SLP performance.

This paper is structured as follows: Section 2 provides some preliminaries, including a review of an existing composite index, an overview of SLPs, and a summary of previous SLP-related PCIs. Section 3 introduces a new composite index for assessing SLP coefficients capability. Section 4 compares the performance of the proposed index with existing methods through simulation. Section 5 presents two real case studies to demonstrate the applicability of the proposed index. Finally, conclusions and remarks for future research are provided in the final section.

II. PRELIMINARIES

The following subsections provide essential definitions that will be used throughout the paper.

A. Traditional Composite Capability Index

Capability index C_{pk} proposed by Kane (1986), is defined as $min\,\{(USL-\mu)/3\sigma\,,(\mu-LSL)/3\sigma\}$. Index C_{pk} has been viewed as a yield-based index since it provides bounds on the process yield for a normally distributed process with a fixed value of C_{pk}. Given a fixed value of C_{pk}, the bounds on process yield P can be expressed as $2\big(3C_{pk}\,\big)-1<p<\big(3C_{pk}\,\big)$ (Boyles, 1991). For instance, if $C_{pk}=1$, then it guarantees that the yield will be not less than 99.73%, or equivalently not more than 2700 ppm of non-conformities. Bothe (1999) proposed a single measure, MC_{pk}, to summarize the capability of several different uncorrelated characteristics on the same part. Given the multiple uncorrelated product characteristics, if every characteristic is within its SLs, the product is capable, while if only one of the characteristics is out of its SLs, it makes the product incapable for the customer. To calculate MC_{pk}, the probability that a measure of the product characteristic is within the SLs (p_i) is firstly obtained for each product characteristic. Consequently, the total proportion of conforming parts (p_{total}) is obtained by Equation (1).

$$p_{total}=\prod_{i=1}^{n}p_i \tag{1}$$

Then, the total proportion of nonconforming parts ($p_{total,NCP}$) can be obtained with the Equation (2).

$$p_{total,NCP}=1-p_{total} \tag{2}$$

Finally, with the inverse cumulative normal distribution function, $\Phi^{-1}(.)$, it is possible to transform $p_{total,NCP}$ into the MC_{pk} by Equation (3).

$$MC_{pk}=\frac{Z_{p_{total,NCP}}}{3} \tag{3}$$

where $Z_{p_{total,NCP}}$ is the corresponding Z value for $p_{total,NCP}$ (Bothe, 1997).

B. Simple Linear Profile and Stable Parameters

Consider a SLP defined by a linear relationship between one response variable and one explanatory variable. For the j^{th} profile sample, we have (X_i,Y_{ij}); $i=1,2,\ldots,n$ and $j=1,2,\ldots,k$. Equation (4) models the relationship between the explanatory and response variables when the process is in-control.

$$Y_{ij}=A_0+A_1X_i+\varepsilon_{ij},\qquad i=1,2,\ldots,n,\qquad j=1,2,\ldots,k. \tag{4}$$

The intercept A_0 and slope A_1 are profile parameters and X_i is explanatory variable with fixed values for each sample. In addition, ε_{ij} are assumed to be independently and identically distributed normal random variables with mean zero and variance σ^2. Therefore, the reference line for the process follows a normal distribution with mean $A_0 + A_1X$ and variance σ^2. The stable values of the parameters A_0 and A_1 must be estimated using in-control profile samples and Equation (5).

$$\hat{A}_0 = a_0 = \frac{\sum_{j=1}^{k} a_{0j}}{k}, \hat{A}_1 = a_1 = \frac{\sum_{j=1}^{k} a_{1j}}{k}. \quad (5)$$

where the least-square estimates of profile parameters for the j^{th} sample calculated by Equation (6) (Kutner et al., 1996).

$$a_{0j} = \bar{Y}_j - a_{1j}\bar{X},\ a_{1j} = \frac{S_{XY(j)}}{S_{XX}}. \quad (6)$$

where $\bar{Y}_j = \frac{\sum_{i=1}^{n} Y_{ij}}{n}, \bar{X} = \frac{\sum_{i=1}^{n} X_i}{n}$, $S_{XY(j)} = \sum_{i=1}^{n}(X_i - \bar{X})Y_{ij}$, $S_{XX} = \sum_{i=1}^{n}(X_i - \bar{X})^2$.

Thus, $\hat{Y}_{ij} = a_{0j} + a_{1j}X_i,\ i = 1, 2, \dots, n$, where $\hat{Y}_{ij}$ denotes the predicted value of the j^{th} response variable for a given level of the explanatory variable. The mean square error is used to estimate the process variance (σ^2) and is calculated as $MSE = \frac{\sum_{j=1}^{k} MSE_j}{k}$, where $MSE_j = \frac{\sum_{i=1}^{n} e_{ij}^2}{(n-2)}$ is the unbiased estimator of σ^2 for sample j and e_{ij} denotes residuals and is defined as $e_{ij} = Y_{ij} - \hat{Y}_{ij}$ (Saghaei and Noorossana, 2011).

C. Overview Of Existing PCI for SLP

(Pakzad et al., 2024) introduced a novel method for evaluating SLP capability that utilizes coded X- values to create independent profile parameters and subsequently proposes two independent univariate indices for profile parameters. Equation (7) represents the transformed version of the SLP model in Equation (4).

"Pakzad et al. (2024)."

$$Y_{ij} = B_0 + B_1X_i' + \varepsilon_{ij},\ i = 1,2, \dots, n, \qquad j = 1,2, \dots, k. \quad (7)$$

where $B_0 = A_0 + A_1\bar{X}$, $B_1 = A_1$ and $X_i' = X_i - \bar{X}$. Similarly, to obtain the stable values of the unknown parameters B_0 and B_1, we can use the in-control profile samples as follows.

$$\hat{B}_0 = b_0 = \frac{\sum_{j=1}^{k} b_{0j}}{k}, \hat{B}_1 = b_1 = \frac{\sum_{j=1}^{k} b_{1j}}{k}. \quad (8)$$

Under this situation, the least-square estimation of profile parameters for the j^{th} sample is calculated using $b_{0j} = \bar{Y}_j$ and $b_{1j} = a_{1j} = \frac{S_{XY(j)}}{S_{XX}}$, respectively. When the process is in-control, both b_{0j} and b_{1j} are mutually independent and follow a normal distribution with means B_0 and B_1 and variances $\frac{\sigma^2}{n}$ and $\frac{\sigma^2}{S_{XX}}$, respectively. This allows for the construction of separate Shewhart control charts using Equations (9) and (10).

$$LCL_{b_0} = b_0 - t_{k(n-2),\frac{\alpha}{2}}\sqrt{\frac{(k-1)MSE}{kn}}, UCL_{b_0} = b_0 + t_{k(n-2),\frac{\alpha}{2}}\sqrt{\frac{(k-1)MSE}{kn}}. \quad (9)$$

$$LCL_{b_1} = b_1 - t_{k(n-2),\frac{\alpha}{2}}\sqrt{\frac{(k-1)MSE}{kS_{XX}}}, UCL_{b_1} = b_1 + t_{k(n-2),\frac{\alpha}{2}}\sqrt{\frac{(k-1)MSE}{kS_{XX}}}. \quad (10)$$

where $t_{k(n-2),\frac{\alpha}{2}}$ is a $100(1-\frac{\alpha}{2})$ percentile of t distribution with $k(n-2)$ degrees of freedom (Kim et al., 2003; Mahmoud and Woodall, 2004). Assuming that the SLs for the reference profile $Y_i = b_0 + b_1X_i'$ at each level of the X_i' are defined by LSL_i and USL_i where $i = 1, 2, \dots, n$, two regression lines can be fitted as shown in Equation (11).

$$USL_i = b_0^{'} + b_1^{'}X_i', LSL_i = b_0^{''} + b_1^{''}X_i'. \quad (11)$$

where $b_0^{'}$, $b_1^{'}$, $b_0^{''}$, and $b_1^{''}$ are the intercepts and slopes for USL_i and LSL_i, respectively. Although the SLs may not be parallel, for simplicity, it is assumed parallelism (Pakzad et al., 2024), so $b_1^{''} = b_1^{'} = b$. Therefore, the SLs based on both a conforming and in-control profile for the intercept and slope were obtained as come in Equations (12) and (13).

$$Min\{b_0^{''} + (b - LCL_{b_1})X_L', b_0^{''} + (b - UCL_{b_1})X_U'\} \le b_0 \le Max\{b_0^{'} + (b - UCL_{b_1})X_L', b_0^{'} + (b - LCL_{b_1})X_U'\}. \quad (12)$$

$$Min\ \{conforming\ \&\ incontrol\ slopes\} \le b_1 \le Max\ \{conforming\ \&\ incontrol\ slopes\}. \quad (13)$$

where X_L' and X_U' are the lower and upper values of X's, and $b + \frac{(b_0^{''} - LCL_{b_0})}{X_U'}$, $b + \frac{(b_0^{'} - UCL_{b_0})}{X_U'}$, $b + \frac{(b_0^{'} - UCL_{b_0})}{X_L'}$ and $b + \frac{(b_0^{''} - LCL_{b_0})}{X_L'}$ are conforming and in-control slopes. Therefore, based on the k in-control profile samples, the estimation of C_{pm} for b_0 and b_1 were defined as Equation (14).

$$\hat{C}_{pm_{b_0}} = \frac{USL_{b_0} - LSL_{b_0}}{6\sqrt{\hat{\sigma}_{b_0}^2 + (\hat{\mu}_{b_0} - T_{b_0})^2}}, \hat{C}_{pm_{b_1}} = \frac{USL_{b_1} - LSL_{b_1}}{6\sqrt{\hat{\sigma}_{b_1}^2 + (\hat{\mu}_{b_1} - T_{b_1})^2}}, \quad (14)$$

The estimated mean and variance of b_0 are denoted by $\hat{\mu}_{b_0} = b_0$ and $\hat{\sigma}_{b_0}^2 = \frac{MSE}{kn}$, respectively. Likewise, the estimated mean and variance of b_1 are represented by $\hat{\mu}_{b_1} = b_1$ and $\hat{\sigma}_{b_1}^2 = \frac{MSE}{kS_{XX}}$. The upper and lower SLs for the intercept and slope are denoted by USL_{b_0}, LSL_{b_0}, USL_{b_1}, and LSL_{b_1}, respectively, and are calculated using Equations (12) and (13). The centers of the SLs for the intercept and slope are T_{b_0} and T_{b_1}, which are also the target values. Both indices $\hat{C}_{pm_{b_0}}$ and $\hat{C}_{pm_{b_1}}$ are used simultaneously to evaluate process capability, and if either index is less than one, the process is deemed "incapable" (Pakzad et al., 2024).

III. NEW CAPABILITY INDEX FOR SIMPLE LINEAR PROFILE

Since the intercept and the slope of SLP can be two-dimensional predictions that describe the prediction profile, a capability index for the SLP considering two-responses (intercept and slope) is developed in this section. For an in-control profile given in Equation (4), it is recommended to use the composite index MC_{pk} proposed by Bothe (1999) for the intercept and slope by employing coded X-values and then the independent profile parameters that follow normal distribution as mentioned in Subsection *C*. Hence, we need to calculate $p_{total,NCP} = 1 - p_{total}$ and p_{total} in order to derive $MC_{pk} = \frac{Z_{p_{total,NCP}}}{3}$ for SLP. In this case, $p_{total} = p_{b_0} . p_{b_1}$, which p_{b_0} and p_{b_1}represent the probability of being within the SLs for the intercept and slope, respectively. These probabilities are obtained using Equations (15) and (16) associated with a normal distribution.

$$p_{b_0} = P\left(LSL_{b_0} \le b_0 \le USL_{b_0}\right). \tag{15}$$

$$p_{b_1} = P\left(LSL_{b_1} \le b_1 \le USL_{b_1}\right). \tag{16}$$

where USL_{b_0}, LSL_{b_0}, USL_{b_1}, and LSL_{b_1} are the upper and lower SLs for the intercept and slope that are calculated based on Equations (12) and (13). The intercept estimator b_0 and the slope estimator b_1 (see Equation (8)) are known to be independent following $N(b_0, \frac{MSE}{kn})$ and $N(b_1, \frac{MSE}{kS_{XX}})$, respectively. It should be noted that the interpretation of the new composite index is the same as that of the traditional ones mentioned in Subsection *A*.

IV. PERFORMANCE OF THE PROPOSED INDEX

To investigate and compare the performance of existing and new capability indices for SLP, we conducted a simulation study in MATLAB. The in-control model given by Kang and Albin (2000), i.e. $Y_{ij} = 3 + 2X_i + \varepsilon_{ij}$, $\varepsilon_{ij} \sim N(0,1)$ with four fixed X_i-values of 2, 4, 6, and 8 is used in the simulation study. In our proposed method, by coding X_i-values, we obtain the transformed model as $Y_{ij} = 13 + 2X_i' + \varepsilon_{ij}$, $\varepsilon_{ij} \sim N(0,1)$ with X_i'-values as -3, -1, 0, 1 and 3. Based on the response SLs for each level of the explanatory variable (as shown in Table I), we fitted two regression lines $USL_i = 16.7125 + 2.2825X_i'$ and $LSL_i = 9.2125 + 2.2825X_i'$, using the transformed model.

Table I. SLs for each level of explanatory variable

i	X_i	LSL_i	USL_i	Target
1	2	2.5	10	6.25
2	4	6.85	14.35	10.60
3	6	11.25	18.75	15
4	8	16.25	23.75	20

We investigate and compare the performance of the proposed index with the existing $C_{pm_{b_0}}$ and $C_{pm_{b_1}}$ indices under different numbers of profile samples ($k \in \{25, 50, 100, 200\}$) and small shifts in intercept, slope, and variance in terms of mean absolute error (MAE) and MSE metrics. For each simulated case, the true values of PCIs are calculated and listed. The number of simulation runs is set to 10,000 to obtain the estimates. In Tables II–IV, the estimated and true values of the MC_{pk}, $C_{pm_{b_0}}$, and $C_{pm_{b_1}}$, as well as the corresponding MAE and MSE values for different simulation cases are reposted. The average values of MAE and MSE for the $C_{pm_{b_0}}$ and $C_{pm_{b_1}}$ are represented by $\overline{MAE}$ and $\overline{MSE}$, respectively. Importantly, the true values of all indices are influenced by the number of profile samples, as this affects the calculation of control limits and, subsequently, the SLs for the intercept and slope. To enhance clarity, the Monte Carlo simulation process used to calculate $\widehat{MC}_{pk}$, MAE, and MSE is detailed in Pseudocode I. This procedure can also be adapted to estimate the existing indices $C_{pm_{b_0}}$ and $C_{pm_{b_1}}$.

Pseudocode I. The procedure for computing MC_{pk}, $\widehat{MC}_{pk}$, MAE, and MSE using Monte Carlo simulation

Consider the in-control transformed profile model (B_0, B_1, σ^2), SLs' function, *n*, *k*, α.

% It is necessary to transfer the SLs as we apply the transformation of the in-control profile model.

% The Monte Carlo simulation loop.

% The computed $\widehat{MC}_{pk}$ in each iteration is denoted by $\widehat{MC}_{pk_{rep}}$, respectively.

for *rep* = 1:1:10,000

Generate *k* profiles with shifts in intercept (λ_{B_0}), slope (λ_{B_1}), standard deviation (λ_{σ^2}).

% The parameter estimation of the transformed model is performed based on the Subsection *C*.

$(b_0. b_1. MSE)$ = Estimate the profile parameters, including the intercept, slope, and process variance using the *k* profiles.

$\left(\delta_{b_0} = b_0 - B_0. \delta_{b_1} = b_1 - B_1. \delta_{\hat{\sigma}^2} = \hat{\sigma}^2 - \sigma^2\right)$ = Compute the estimation error of each profile parameters, including the intercept, slope, and standard deviation.

Compute UCL_{b_0}, LCL_{b_0}, UCL_{b_1}, and LCL_{b_1} based on Eqs. (9) and (10) and the in-control parameters $(B_0. B_1. \sigma^2)$.

Compute USL_{b_0}, LSL_{b_0}, USL_{b_1}, and LSL_{b_1} based on Eqs. (12) and (13).

Compute p_{b_0}, and p_{b_1} based on Eqs. (15) and (16) and considering shifts in parameters $\left(\lambda_{B_0} . \lambda_{B_1} . \lambda_{\sigma^2}\right)$

Compute $p_{total} = p_{b_0}, p_{b_1}$, $p_{total,NCP} = 1 - p_{total}$, and $MC_{pk} = \frac{z_{p_{total,NCP}}}{3}$.

Compute $\widehat{UCL}_{b_0}$, $\widehat{LCL}_{b_0}$, $\widehat{UCL}_{b_1}$, and $\widehat{LCL}_{b_1}$ based on Eqs. (9) and (10) by b_0, b_1, and MSE .

Compute $\widehat{USL}_{b_0}$, $\widehat{LSL}_{b_0}$, $\widehat{USL}_{b_1}$, and $\widehat{LSL}_{b_1}$ based on Eqs. (12) and (13).

Compute $\hat{p}_{b_0}$, and $\hat{p}_{b_1}$ based on Eqs. (15) and (16) and considering shifts in parameters $\left(\lambda_{B_0}, \lambda_{B_1}, \lambda_{\sigma^2}\right)$

Compute $\hat{p}_{total} = \hat{p}_{b_0}, \hat{p}_{b_1}$, $\hat{p}_{total,NCP} = 1 - \hat{p}_{total}$, and $\widehat{MC}_{pk_{rep}} = \frac{\hat{z}_{p_{total,NCP}}}{3}$.

Store the values $\widehat{MC}_{pk_{rep}}$

Store the values $\left| \widehat{MC}_{pk_{rep}} - MC_{pk} \right|$

Store the values $(\widehat{MC}_{pk_{rep}} - MC_{pk})^2$

end for

$\widehat{MC}_{pk} = \frac{\sum_{rep=1}^{10,000} \widehat{MC}_{pk_{rep}}}{10,000}$.

MAE $= \frac{\sum_{rep=1}^{10,000} \left| \widehat{MC}_{pk_{rep}} - MC_{pk} \right|}{10,000}$.

MSE $= \frac{\sum_{rep=1}^{10,000} (\widehat{MC}_{pk_{rep}} - MC_{pk})^2}{10,000}$.

Table II. Simulation results for small shifts in B_0 parameter

Simulated case	k	C_{pm}				C_{pm}	MC_{pk}	
		$C_{pm_{b_0}}$		$C_{pm_{b_1}}$				
		True value	Estimated $(MAE_{C_{pm_{b_0}}}, MSE_{C_{pm_{b_0}}})$	True value	Estimated $(MAE_{C_{pm_{b_1}}}, MSE_{C_{pm_{b_1}}})$	$(\overline{MAE}, \overline{MSE})$	True value	Estimated (MAE, MSE)
$Y_{ij} = 13.15 + 2X_i' + \varepsilon_{ij}$	25	4.356	4.335 (0.294, 0.137)	0.621	0.645 (0.083, 0.012)	(0.189, 0.074)	0.579	0.624 (0.137, 0.031)
	50	4.407	4.396 (0.212, 0.071)	0.602	0.615 (0.058, 0.006)	(0.135, 0.038)	0.549	0.572 (0.095, 0.014)
	100	4.466	4.459 (0.153, 0.037)	0.580	0.588 (0.041, 0.003)	(0.097, 0.020)	0.514	0.527 (0.067, 0.007)
	200	4.528	4.527 (0.108, 0.018)	0.558	0.560 (0.029, 0.001)	(0.069, 0.010)	0.477	0.482 (0.047, 0.004)
$Y_{ij} = 13.1 + 2X_i' + \varepsilon_{ij}$	25	4.485	4.456 (0.284, 0.129)	0.621	0.646 (0.085, 0.012)	(0.184, 0.070)	0.579	0.624 (0.138, 0.032)
	50	4.538	4.527 (0.204, 0.065)	0.602	0.616 (0.059, 0.006)	(0.131, 0.035)	0.549	0.575 (0.096, 0.015)
	100	4.599	4.591 (0.146, 0.034)	0.580	0.587 (0.041, 0.003)	(0.093, 0.018)	0.514	0.526 (0.067, 0.007)
	200	4.663	4.658 (0.103, 0.017)	0.558	0.561 (0.029, 0.001)	(0.066, 0.009)	0.477	0.482 (0.047, 0.003)
$Y_{ij} = 13 + 2X_i' + \varepsilon_{ij}$	25	4.639	4.597 (0.266, 0.112)	0.621	0.645 (0.083, 0.012)	(0.175, 0.062)	0.579	0.624 (0.137, 0.031)
	50	4.694	4.669 (0.185, 0.054)	0.602	0.615 (0.058, 0.005)	(0.121, 0.030)	0.549	0.572 (0.094, 0.014)
	100	4.756	4.744 (0.130, 0.027)	0.580	0.587 (0.041, 0.003)	(0.086, 0.015)	0.514	0.526 (0.067, 0.007)
	200	4.822	4.815 (0.092, 0.013)	0.558	0.560 (0.029, 0.001)	(0.060, 0.007)	0.477	0.482 (0.047, 0.004)
$Y_{ij} = 12.9 + 2X_i' + \varepsilon_{ij}$	25	4.616	4.573 (0.269, 0.115)	0.621	0.646 (0.083, 0.012)	(0.176, 0.063)	0.579	0.624 (0.136, 0.031)
	50	4.671	4.650 (0.187, 0.056)	0.602	0.615 (0.058, 0.006)	(0.123, 0.031)	0.549	0.572 (0.095, 0.015)
	100	4.733	4.721 (0.133, 0.028)	0.580	0.587 (0.041, 0.003)	(0.087, 0.015)	0.514	0.525 (0.066, 0.007)
	200	4.798	4.795 (0.095, 0.014)	0.558	0.560 (0.029, 0.001)	(0.062, 0.008)	0.477	0.483 (0.047, 0.004)
$Y_{ij} = 12.85 + 2X_i' + \varepsilon_{ij}$	25	4.538	4.505 (0.280, 0.126)	0.621	0.648 (0.085, 0.012)	(0.182, 0.069)	0.579	0.627 (0.140, 0.033)
	50	4.592	4.574 (0.201, 0.064)	0.603	0.615 (0.059, 0.006)	(0.130, 0.035)	0.549	0.572 (0.096, 0.015)
	100	4.653	4.644 (0.138, 0.030)	0.580	0.587 (0.040, 0.003)	(0.089, 0.016)	0.514	0.526 (0.065, 0.007)
	200	4.718	4.713 (0.099, 0.015)	0.558	0.560 (0.029, 0.001)	(0.064, 0.008)	0.477	0.482 (0.047, 0.004)

Table III. Simulation results for small shifts in B_1 parameter

Simulated case	k	C_{pm}				C_{pm}	MC_{pk}	
		$C_{pm_{b_0}}$		$C_{pm_{b_1}}$				
		True value	Estimated ($MAE_{C_{pm_{b_0}}}, MSE_{C_{pm_{b_0}}}$)	True value	Estimated ($MAE_{C_{pm_{b_1}}}, MSE_{C_{pm_{b_1}}}$)	($\overline{MAE}$,$\overline{MSE}$)	True value	Estimated (MAE, MSE)
$Y_{ij} = 13 + 2.15X_i' + \varepsilon_{ij}$	25	4.639	4.593 (0.272, 0.117)	0.861	0.895 (0.132, 0.029)	(0.202, 0.073)	0.801	0.847 (0.156, 0.040)
	50	4.694	4.670 (0.184, 0.054)	0.834	0.852 (0.092, 0.013)	(0.138, 0.033)	0.770	0.793 (0.107, 0.018)
	100	4.756	4.742 (0.129, 0.026)	0.804	0.813 (0.064, 0.007)	(0.097, 0.016)	0.734	0.746 (0.075, 0.009)
	200	4.822	4.816 (0.092, 0.013)	0.773	0.777 (0.045, 0.003)	(0.068, 0.008)	0.697	0.702 (0.053, 0.004)
$Y_{ij} = 13 + 2.1X_i' + \varepsilon_{ij}$	25	4.639	4.597 (0.266, 0.112)	0.775	0.806 (0.114, 0.022)	(0.190, 0.067)	0.728	0.774 (0.148, 0.036)
	50	4.694	4.669 (0.185, 0.054)	0.751	0.768 (0.080, 0.010)	(0.132, 0.032)	0.697	0.721 (0.102, 0.017)
	100	4.756	4.744 (0.130, 0.027)	0.724	0.733 (0.057, 0.005)	(0.093, 0.016)	0.662	0.675 (0.073, 0.009)
	200	4.822	4.815 (0.092, 0.013)	0.696	0.700 (0.040, 0.003)	(0.066, 0.008)	0.625	0.630 (0.051, 0.004)
$Y_{ij} = 13 + 2X_i' + \varepsilon_{ij}$	25	4.639	4.597 (0.266, 0.112)	0.621	0.645 (0.083, 0.012)	(0.175, 0.062)	0.579	0.624 (0.137, 0.031)
	50	4.694	4.669 (0.185, 0.054)	0.602	0.615 (0.058, 0.005)	(0.121, 0.030)	0.549	0.572 (0.094, 0.014)
	100	4.756	4.744 (0.130, 0.027)	0.580	0.587 (0.041, 0.003)	(0.086, 0.015)	0.514	0.526 (0.067, 0.007)
	200	4.822	4.815 (0.092, 0.013)	0.558	0.560 (0.029, 0.001)	(0.060, 0.007)	0.477	0.482 (0.047, 0.004)
$Y_{ij} = 13 + 1.9X_i' + \varepsilon_{ij}$	25	4.639	4.599 (0.267, 0.113)	0.505	0.524 (0.061, 0.006)	(0.164, 0.060)	0.430	0.474 (0.126, 0.027)
	50	4.694	4.674 (0.184, 0.054)	0.489	0.499 (0.043, 0.003)	(0.114, 0.028)	0.400	0.423 (0.088, 0.013)
	100	4.756	4.746 (0.132, 0.028)	0.472	0.477 (0.030, 0.001)	(0.081, 0.015)	0.365	0.377 (0.061, 0.006)
	200	4.822	4.815 (0.092, 0.013)	0.453	0.455 (0.021, 0.001)	(0.057, 0.007)	0.328	0.337 (0.043, 0.003)
$Y_{ij} = 13 + 1.85X_i' + \varepsilon_{ij}$	25	4.639	4.599 (0.266, 0.112)	0.460	0.478 (0.054, 0.005)	(0.160, 0.059)	0.356	0.402 (0.122, 0.025)
	50	4.694	4.667 (0.184, 0.053)	0.445	0.453 (0.037, 0.002)	(0.111, 0.028)	0.325	0.345 (0.084, 0.011)
	100	4.756	4.744 (0.131, 0.027)	0.429	0.434 (0.027, 0.001)	(0.079, 0.014)	0.290	0.302 (0.060, 0.006)
	200	4.822	4.816 (0.092, 0.013)	0.413	0.415 (0.019, 0.001)	(0.056, 0.007)	0.254	0.259 (0.042, 0.003)

Table IV. Simulation results for small shifts in σ^2 parameter

Simulated case	k	C_{pm}				C_{pm}	MC_{pk}	
		$C_{pm_{b_0}}$		$C_{pm_{b_1}}$				
		True value	Estimated ($MAE_{C_{pm_{b_0}}}$, $MSE_{C_{pm_{b_0}}}$)	True value	Estimated ($MAE_{C_{pm_{b_1}}}$, $MSE_{C_{pm_{b_1}}}$)	($\overline{MAE}$,$\overline{MSE}$)	True value	Estimated (MAE, MSE)
$\varepsilon_{ij} \sim N(0,(0.8)^2)$	25	5.183	5.156 (0.405, 0.273)	0.646	0.675 (0.091, 0.014)	(0.248, 0.144)	0.648	0.710 (0.169, 0.050)
	50	5.244	5.233 (0.283, 0.129)	0.627	0.642 (0.064, 0.007)	(0.173, 0.068)	0.613	0.646 (0.117, 0.023)
	100	5.314	5.306 (0.196, 0.061)	0.604	0.611 (0.044, 0.003)	(0.120, 0.032)	0.575	0.590 (0.080, 0.010)
	200	5.388	5.382 (0.141, 0.031)	0.580	0.584 (0.031, 0.002)	(0.086, 0.016)	0.534	0.540 (0.056, 0.005)
$\varepsilon_{ij} \sim N(0,(0.9)^2)$	25	4.888	4.842 (0.327, 0.170)	0.633	0.661 (0.088, 0.013)	(0.207, 0.091)	0.611	0.663 (0.151, 0.039)
	50	4.946	4.929 (0.227, 0.081)	0.614	0.629 (0.061, 0.006)	(0.144, 0.044)	0.578	0.607 (0.104, 0.018)
	100	5.012	5.001 (0.157, 0.039)	0.592	0.599 (0.043, 0.003)	(0.100, 0.021)	0.542	0.555 (0.073, 0.008)
	200	5.081	5.076 (0.112, 0.020)	0.569	0.571 (0.030, 0.001)	(0.071, 0.011)	0.503	0.509 (0.051, 0.004)
$\varepsilon_{ij} \sim N(0,(1.0)^2)$	25	4.639	4.597 (0.266, 0.112)	0.621	0.645 (0.083, 0.012)	(0.175, 0.062)	0.579	0.624 (0.137, 0.031)
	50	4.694	4.669 (0.185, 0.054)	0.602	0.615 (0.058, 0.005)	(0.121, 0.030)	0.549	0.572 (0.094, 0.014)
	100	4.756	4.744 (0.130, 0.027)	0.580	0.587 (0.041, 0.003)	(0.086, 0.015)	0.514	0.526 (0.067, 0.007)
	200	4.822	4.815 (0.092, 0.013)	0.558	0.560 (0.029, 0.001)	(0.060, 0.007)	0.477	0.482 (0.047, 0.004)
$\varepsilon_{ij} \sim N(0,(1.1)^2)$	25	4.424	4.377 (0.223, 0.078)	0.609	0.633 (0.081, 0.011)	(0.152, 0.045)	0.552	0.594 (0.128, 0.027)
	50	4.477	4.457 (0.156, 0.038)	0.591	0.604 (0.057, 0.005)	(0.106, 0.022)	0.523	0.547 (0.089, 0.013)
	100	4.536	4.526 (0.109, 0.019)	0.570	0.576 (0.039, 0.002)	(0.074, 0.011)	0.490	0.501 (0.062, 0.006)
	200	4.599	4.594 (0.075, 0.009)	0.547	0.550 (0.028, 0.001)	(0.052, 0.005)	0.455	0.460 (0.044, 0.003)
$\varepsilon_{ij} \sim N(0,(1.2)^2)$	25	4.237	4.194 (0.193, 0.058)	0.598	0.621 (0.078, 0.010)	(0.135, 0.034)	0.529	0.566 (0.118, 0.023)
	50	4.287	4.262 (0.130, 0.026)	0.580	0.592 (0.055, 0.005)	(0.092, 0.016)	0.501	0.520 (0.083, 0.011)
	100	4.344	4.332 (0.093, 0.014)	0.559	0.566 (0.038, 0.002)	(0.066, 0.008)	0.469	0.480 (0.058, 0.005)
	200	4.404	4.398 (0.064, 0.007)	0.537	0.540 (0.027, 0.001)	(0.045, 0.004)	0.435	0.439 (0.041, 0.003)

According to performance assessment metrics results in Tables II–IV, the proposed index MC_{pk} consistently outperforms the existing indices $C_{pm_{b_0}}$ and $C_{pm_{b_1}}$ in terms of both MAE and MSE across all simulated scenarios. This superiority is evident in the lower MAE and MSE values associated with the proposed index, as highlighted in Tables II-IV. Also, it can be seen that the number of profile samples k affects the estimates of all PCIs. So that, as the number of profiles in the sample increases, the values of MAE and MSE decrease, and the estimates improve. Based on another simulation result provided in Tables II and III, the values of the proposed index MC_{pk} is more sensitive to small shifts in the slope compared to the intercept. Additionally, Table IV shows that as σ^2 decreases, the values of MC_{pk} increase, and vice versa.

To provide a more comprehensive assessment, the performance of the indices was evaluated under scenarios where simultaneous small shifts occur in the B_0 and B_1 under different error term variances, as shown in Tables V-VII and Figures I-III. While all PCIs generally improve with larger profile sample sizes, the proposed index consistently outperforms the existing method across various simulation scenarios and sample size k. Notably, as Figures I–III demonstrate, the superiority of the proposed index is especially evident in cases involving smaller sample sizes. This characteristic is particularly advantageous in real-world situations, where obtaining large sample sizes is often constrained. Therefore, we propose using the index MC_{pk} to assess the process capability of SLP processes based on its parameters.

Table V. Simulation results for $\varepsilon_{ij} \sim N(0, (0.8)^2)$ and small shifts in B_0 and B_1 parameter

Simulated case	k	C_{pm}				C_{pm}	MC_{pk}	
		$C_{pm_{b_0}}$		$C_{pm_{b_1}}$				
		True value	Estimated $(MAE_{C_{pm_{b_0}}}, MSE_{C_{pm_{b_0}}})$	True value	Estimated $(MAE_{C_{pm_{b_1}}}, MSE_{C_{pm_{b_1}}})$	$(\overline{MAE}, \overline{MSE})$	True value	Estimated (MAE, MSE)
$Y_{ij} = 13.2 + 2.2X_i' + \varepsilon_{ij}$	25	4.593	4.598 (0.410, 0.273)	1.034	1.077 (0.180, 0.055)	(0.295, 0.164)	0.976	1.035 (0.203, 0.070)
	50	4.648	4.652 (0.295, 0.140)	1.002	1.026 (0.125, 0.026)	(0.210, 0.083)	0.941	0.972 (0.139, 0.032)
	100	4.710	4.713 (0.215, 0.073)	0.966	0.979 (0.087, 0.012)	(0.151, 0.042)	0.902	0.917 (0.096, 0.015)
	200	4.775	4.778 (0.149, 0.035)	0.929	0.933 (0.061, 0.006)	(0.105, 0.021)	0.860	0.865 (0.068, 0.007)
$Y_{ij} = 12.95 + 2.1X_i' + \varepsilon_{ij}$	25	5.199	5.173 (0.401, 0.259)	0.826	0.866 (0.134, 0.031)	(0.268, 0.145)	0.814	0.881 (0.187, 0.060)
	50	5.261	5.241 (0.282, 0.127)	0.801	0.821 (0.093, 0.014)	(0.187, 0.070)	0.780	0.812 (0.127, 0.027)
	100	5.331	5.322 (0.198, 0.062)	0.772	0.782 (0.064, 0.007)	(0.131, 0.034)	0.741	0.758 (0.088, 0.013)
	200	5.404	5.397 (0.139, 0.030)	0.742	0.746 (0.045, 0.003)	(0.092, 0.017)	0.700	0.706 (0.061, 0.006)
$Y_{ij} = 13.1 + 1.85X_i' + \varepsilon_{ij}$	25	4.971	4.956 (0.413, 0.283)	0.470	0.488 (0.056, 0.005)	(0.235, 0.144)	0.398	0.455 (0.147, 0.038)
	50	5.030	5.024 (0.292, 0.137)	0.455	0.464 (0.039, 0.003)	(0.166, 0.070)	0.363	0.392 (0.100, 0.017)
	100	5.097	5.091 (0.210, 0.069)	0.439	0.444 (0.027, 0.001)	(0.118, 0.035)	0.325	0.339 (0.068, 0.007)
	200	5.168	5.168 (0.147, 0.034)	0.422	0.423 (0.020, 0.001)	(0.083, 0.017)	0.284	0.290 (0.049, 0.004)
$Y_{ij} = 13.2 + 1.8X_i' + \varepsilon_{ij}$	25	4.593	4.600 (0.410, 0.276)	0.428	0.444 (0.049, 0.004)	(0.230, 0.140)	0.314	0.369 (0.141, 0.034)
	50	4.648	4.654 (0.294, 0.141)	0.415	0.423 (0.034, 0.002)	(0.164, 0.071)	0.280	0.307 (0.093, 0.014)
	100	4.710	4.712 (0.214, 0.073)	0.400	0.404 (0.024, 0.001)	(0.119, 0.037)	0.241	0.255 (0.065, 0.007)
	200	4.775	4.772 (0.151, 0.036)	0.385	0.386 (0.017, 0.001)	(0.084, 0.018)	0.200	0.205 (0.046, 0.003)
$Y_{ij} = 12.8 + 1.8X_i' + \varepsilon_{ij}$	25	4.888	4.889 (0.419, 0.289)	0.428	0.444 (0.050, 0.004)	(0.234, 0.147)	0.314	0.369 (0.141, 0.034)
	50	4.946	4.944 (0.293, 0.138)	0.415	0.423 (0.034, 0.002)	(0.163, 0.070)	0.280	0.308 (0.095, 0.015)
	100	5.012	5.007 (0.211, 0.072)	0.400	0.404 (0.024, 0.001)	(0.118, 0.036)	0.241	0.255 (0.066, 0.007)
	200	5.081	5.081 (0.150, 0.036)	0.385	0.386 (0.017, 0.001)	(0.084, 0.018)	0.200	0.206 (0.045, 0.003)

Table VI. Simulation results for $\varepsilon_{ij} \sim N(0.(1.0)^2)$ and small shifts in B_0 and B_1 parameter

Simulated case	k	C_{pm}				C_{pm}	MC_{pk}	
		$C_{pm_{b_0}}$		$C_{pm_{b_1}}$				
		True value	Estimated $(MAE_{C_{pm_{b_0}}}, MSE_{C_{pm_{b_0}}})$	True value	Estimated $(MAE_{C_{pm_{b_1}}}, MSE_{C_{pm_{b_1}}})$	$(\overline{MAE}, \overline{MSE})$	True value	Estimated (MAE, MSE)
$Y_{ij} = 13.2 + 2.2X_i' + \varepsilon_{ij}$	25	4.202	4.189 (0.301, 0.144)	0.939	0.968 (0.145, 0.035)	(0.223, 0.089)	0.868	0.906 (0.160, 0.042)
	50	4.252	4.243 (0.218, 0.075)	0.910	0.928 (0.102, 0.017)	(0.160, 0.046)	0.836	0.858 (0.112, 0.020)
	100	4.308	4.305 (0.158, 0.039)	0.877	0.887 (0.073, 0.008)	(0.116, 0.024)	0.800	0.813 (0.081, 0.010)
	200	4.368	4.367 (0.113, 0.020)	0.843	0.847 (0.051, 0.004)	(0.082, 0.012)	0.762	0.767 (0.056, 0.005)
$Y_{ij} = 12.95 + 2.1X_i' + \varepsilon_{ij}$	25	4.650	4.609 (0.271, 0.115)	0.775	0.808 (0.117, 0.023)	(0.194, 0.069)	0.728	0.776 (0.151, 0.038)
	50	4.706	4.685 (0.185, 0.055)	0.751	0.768 (0.081, 0.011)	(0.133, 0.033)	0.697	0.722 (0.104, 0.018)
	100	4.768	4.755 (0.129, 0.026)	0.724	0.733 (0.056, 0.005)	(0.093, 0.016)	0.662	0.674 (0.072, 0.008)
	200	4.834	4.827 (0.092, 0.013)	0.696	0.700 (0.040, 0.003)	(0.066, 0.008)	0.625	0.631 (0.051, 0.004)
$Y_{ij} = 13.1 + 1.85X_i' + \varepsilon_{ij}$	25	4.485	4.461 (0.285, 0.129)	0.460	0.476 (0.053, 0.005)	(0.169, 0.067)	0.356	0.399 (0.120, 0.024)
	50	4.539	4.527 (0.202, 0.065)	0.445	0.455 (0.038, 0.002)	(0.120, 0.033)	0.325	0.350 (0.085, 0.012)
	100	4.599	4.588 (0.142, 0.032)	0.429	0.434 (0.026, 0.001)	(0.084, 0.017)	0.290	0.301 (0.059, 0.006)
	200	4.663	4.658 (0.102, 0.016)	0.413	0.414 (0.019, 0.001)	(0.061, 0.009)	0.254	0.258 (0.042, 0.003)
$Y_{ij} = 13.2 + 1.8X_i' + \varepsilon_{ij}$	25	4.202	4.193 (0.304, 0.146)	0.421	0.435 (0.047, 0.004)	(0.176, 0.075)	0.281	0.322 (0.117, 0.023)
	50	4.252	4.248 (0.220, 0.076)	0.408	0.416 (0.033, 0.002)	(0.126, 0.039)	0.251	0.274 (0.081, 0.011)
	100	4.308	4.305 (0.158, 0.039)	0.393	0.397 (0.023, 0.001)	(0.091, 0.020)	0.216	0.227 (0.056, 0.005)
	200	4.368	4.365 (0.112, 0.020)	0.378	0.379 (0.017, 0.000)	(0.064, 0.010)	0.179	0.184 (0.040, 0.003)
$Y_{ij} = 12.8 + 1.8X_i' + \varepsilon_{ij}$	25	4.424	4.405 (0.292, 0.136)	0.421	0.435 (0.047, 0.004)	(0.169, 0.070)	0.281	0.322 (0.116, 0.022)
	50	4.477	4.460 (0.206, 0.067)	0.408	0.416 (0.033, 0.002)	(0.119, 0.035)	0.251	0.272 (0.080, 0.010)
	100	4.536	4.530 (0.150, 0.036)	0.393	0.398 (0.023, 0.001)	(0.087, 0.018)	0.216	0.228 (0.057, 0.005)
	200	4.599	4.595 (0.105, 0.018)	0.378	0.380 (0.017, 0.000)	(0.061, 0.009)	0.179	0.184 (0.040, 0.003)

Table VII. Simulation results for $\varepsilon_{ij} \sim N(0.(1.2)^2)$ and small shifts in B_0 and B_1 parameter

Simulated case	k	C_{pm}				C_{pm}	MC_{pk}	
		$C_{pm_{b_0}}$		$C_{pm_{b_1}}$				
		True value	Estimated ($MAE_{C_{pm_{b_0}}}, MSE_{C_{pm_{b_0}}}$)	True value	Estimated ($MAE_{C_{pm_{b_1}}}, MSE_{C_{pm_{b_1}}}$)	($\overline{MAE}$,$\overline{MSE}$)	True value	Estimated (MAE, MSE)
$Y_{ij} = 13.2 + 2.2X_i' + \varepsilon_{ij}$	25	3.896	3.877 (0.239, 0.089)	0.866	0.895 (0.124, 0.025)	(0.181, 0.057)	0.786	0.822 (0.137, 0.030)
	50	3.942	3.931 (0.169, 0.045)	0.839	0.855 (0.086, 0.012)	(0.128, 0.029)	0.757	0.775 (0.095, 0.014)
	100	3.995	3.994 (0.122, 0.023)	0.809	0.816 (0.062, 0.006)	(0.092, 0.015)	0.724	0.732 (0.068, 0.007)
	200	4.050	4.051 (0.088, 0.012)	0.777	0.780 (0.043, 0.003)	(0.066, 0.008)	0.689	0.692 (0.048, 0.004)
$Y_{ij} = 12.95 + 2.1X_i' + \varepsilon_{ij}$	25	4.245	4.201 (0.192, 0.058)	0.732	0.762 (0.104, 0.018)	(0.148, 0.038)	0.663	0.704 (0.129, 0.027)
	50	4.296	4.269 (0.131, 0.027)	0.710	0.724 (0.071, 0.008)	(0.101, 0.017)	0.635	0.655 (0.088, 0.012)
	100	4.353	4.342 (0.090, 0.013)	0.685	0.693 (0.050, 0.004)	(0.070, 0.007)	0.603	0.614 (0.062, 0.006)
	200	4.413	4.408 (0.063, 0.006)	0.658	0.661 (0.035, 0.002)	(0.049, 0.004)	0.569	0.573 (0.044, 0.003)
$Y_{ij} = 13.1 + 1.85X_i' + \varepsilon_{ij}$	25	4.119	4.088 (0.211, 0.071)	0.450	0.468 (0.053, 0.005)	(0.132, 0.038)	0.325	0.364 (0.109, 0.019)
	50	4.168	4.152 (0.150, 0.036)	0.436	0.444 (0.036, 0.002)	(0.093, 0.019)	0.297	0.315 (0.074, 0.009)
	100	4.223	4.213 (0.105, 0.018)	0.421	0.425 (0.025, 0.001)	(0.065, 0.009)	0.265	0.274 (0.052, 0.004)
	200	4.282	4.277 (0.076, 0.009)	0.404	0.406 (0.018, 0.001)	(0.047, 0.005)	0.232	0.236 (0.037, 0.002)
$Y_{ij} = 13.2 + 1.8X_i' + \varepsilon_{ij}$	25	3.896	3.879 (0.238, 0.088)	0.413	0.428 (0.045, 0.003)	(0.142, 0.046)	0.257	0.292 (0.102, 0.017)
	50	3.942	3.938 (0.169, 0.045)	0.401	0.408 (0.032, 0.002)	(0.100, 0.023)	0.229	0.248 (0.071, 0.008)
	100	3.995	3.990 (0.122, 0.023)	0.386	0.390 (0.023, 0.001)	(0.072, 0.012)	0.197	0.207 (0.051, 0.004)
	200	4.050	4.047 (0.087, 0.012)	0.371	0.373 (0.016, 0.000)	(0.052, 0.006)	0.164	0.167 (0.036, 0.002)
$Y_{ij} = 12.8 + 1.8X_i' + \varepsilon_{ij}$	25	4.071	4.043 (0.220, 0.077)	0.413	0.429 (0.045, 0.003)	(0.133, 0.040)	257	0.294 (0.103, 0.017)
	50	4.120	4.107 (0.157, 0.039)	0.401	0.409 (0.032, 0.002)	(0.095, 0.020)	0.229	0.248 (0.072, 0.008)
	100	4.174	4.167 (0.111, 0.019)	0.386	0.390 (0.022, 0.001)	(0.067, 0.010)	0.197	0.205 (0.050, 0.004)
	200	4.232	4.227 (0.079, 0.010)	0.371	0.373 (0.016, 0.000)	(0.048, 0.005)	0.164	0.168 (0.036, 0.002)

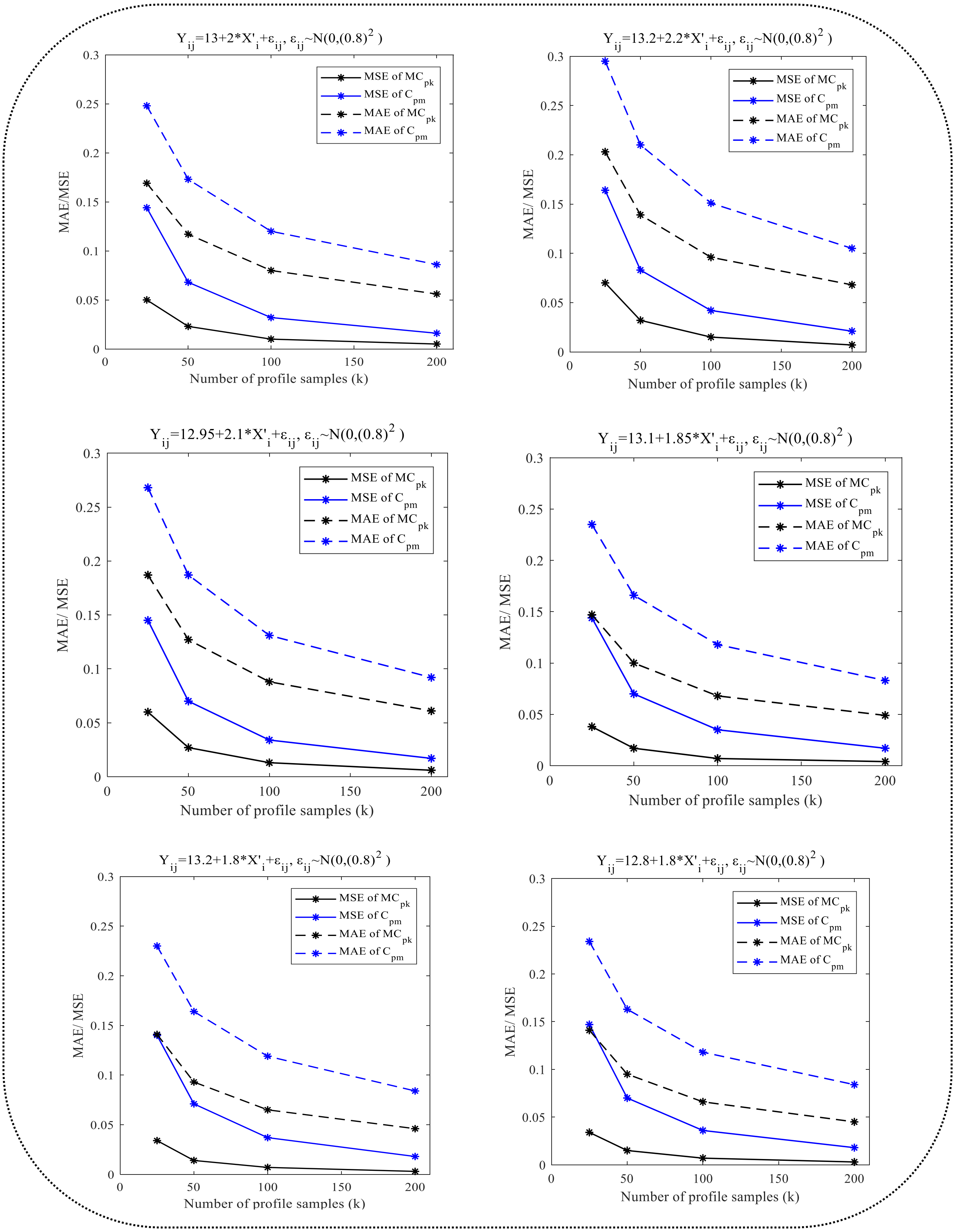

Fig. 1. The values of MAE/ MSE in $k \in \{25, 50, 100, 200\}$for $\varepsilon_{ij} \sim N(0.(0.8)^2)$ and small shifts in B_0 and B_1.

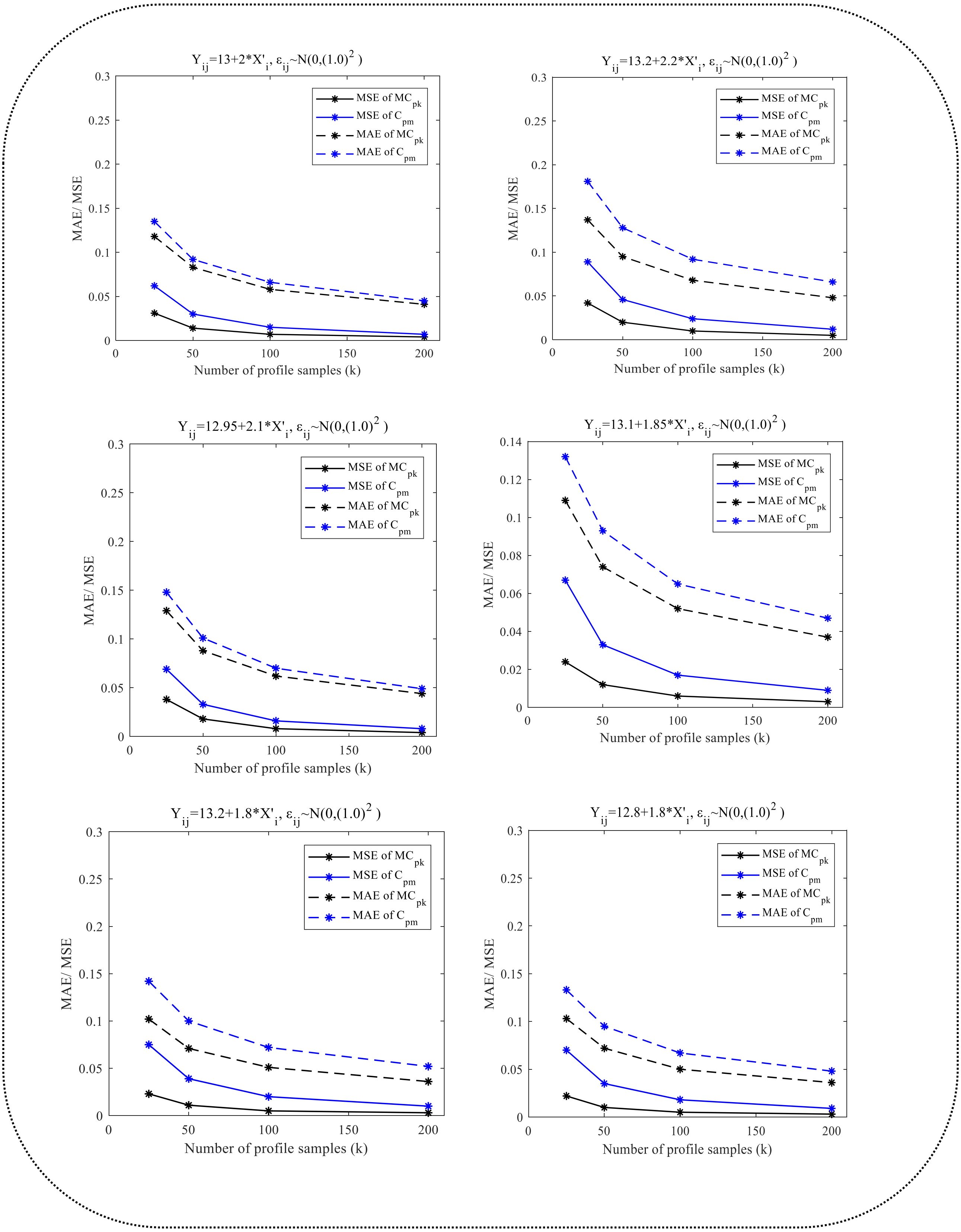

Fig. 2. The values of MAE/ MSE in $k \in \{25, 50, 100, 200\}$for $\varepsilon_{ij} \sim N(0. (1.0)^2)$ and small shifts in B_0 and B_1.

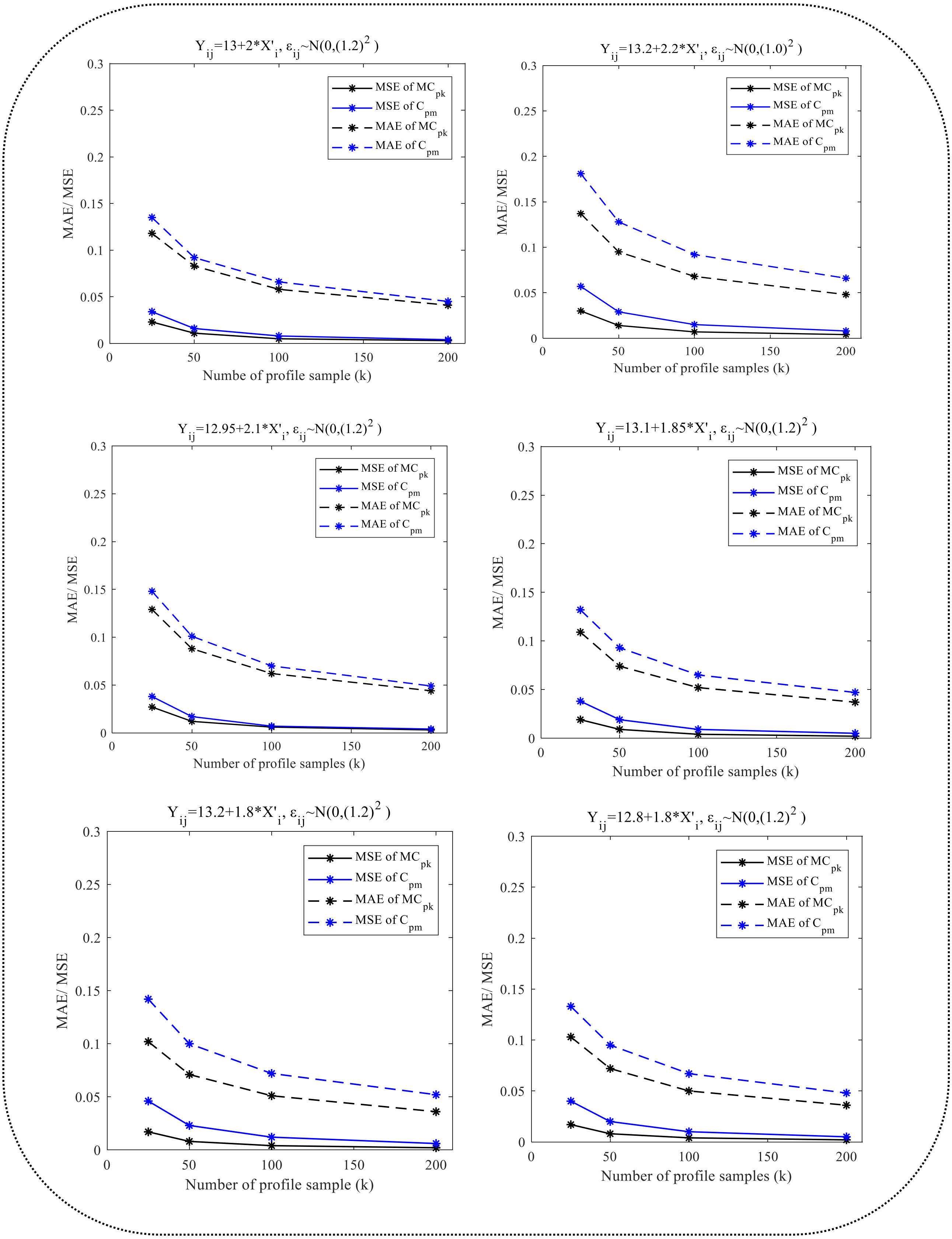

Fig. 3. The values of MAE/ MSE in $k \in \{25, 50, 100, 200\}$for $\varepsilon_{ij} \sim N(0.(1.2)^2)$ and small shifts in B_0 and B_1.

V. REAL CASE

This section presents two case studies to illustrate the application of our proposed method.

A. Example 1

To illustrate the application of our proposed method, we consider a case study originally presented by Natrella (2010) and further analyzed by Wang and Tamirat (2014) and Pakzad et al. (2024). This case study involves monitoring the line widths of three photomask reference standards. To calibrate the optical imaging system, three control measurements were taken for each standard at the lower, middle, and upper ends of the calibration interval. The initial calibration experiment included 10 units (40 measurements) and resulted in an in-control linear calibration profile $Y_{ij} = 0.2357 + 0.9870\, X_i + \varepsilon_{ij}$ with a residual standard deviation of 0.06203. The SLs for the response variable at each level of the explanatory variable are provided in Table VIII.

Table VIII. Line-width SLs at each measurement level (Wang and Tamirat, 2014)

i	X_i	LSL_i	USL_i	Target
1	0.76	0.70	1.30	1.024
2	3.29	3.20	3.80	3.495
3	8.89	8.70	9.30	8.965

To evaluate the capability of the calibration process for the optical imaging system based on the proposed method, we used two simulated datasets of size $k = 50$ profiles, generated by Pakzad et al. (2024). These datasets were based on the same model and residual standard deviations as used by Wang and Tamirat (2014) to represent incapable and capable processes. Tables IX and X show the simulated data for the incapable and capable processes, respectively. Then, the transformed model for both incapable and capable processes, as well as profile SLs are obtained as $Y_{ij} = 4.5 + 0.9870X_i'$, $LSL_i = 4.2 + 0.9837X_i'$, and $USL_i = 4.8 + 0.9837X_i'$, respectively.

Table IX. Simulated data for 50 incapable line-width profiles (Pakzad et al., 2024)

NO.	y_1	NO.	y_1	NO.	y_2	NO.	y_2	NO.	y_3	NO.	y_3
1	1.039029	26	1.088235	1	3.397398	26	3.344075	1	9.093297	26	8.983126
2	1.167355	27	1.057762	2	3.490559	27	3.342085	2	8.922185	27	9.118844
3	0.762174	28	0.955759	3	3.362702	28	3.531231	3	9.020009	28	8.982591
4	1.071155	29	1.014893	4	3.372663	29	3.46534	4	8.956192	29	9.079553
5	1.017358	30	0.907859	5	3.482222	30	3.463491	5	9.040149	30	8.80697
6	0.856339	31	1.073751	6	3.63463	31	3.623412	6	8.950668	31	8.975069
7	0.942874	32	0.87224	7	3.406703	32	3.511767	7	9.058607	32	8.928565
8	1.01972	33	0.879982	8	3.519667	33	3.502483	8	9.083297	33	8.853971
9	1.340061	34	0.90566	9	3.460567	34	3.640082	9	9.179577	34	9.060389
10	1.259974	35	0.694316	10	3.593518	35	3.403258	10	8.990882	35	9.038016
11	0.852161	36	1.1282	11	3.375083	36	3.551866	11	8.798403	36	9.013415
12	1.286257	37	1.017994	12	3.486123	37	3.565574	12	8.926981	37	8.878066
13	1.057615	38	0.911062	13	3.5376	38	3.458772	13	9.144205	38	9.121722

Continue Table IX. Simulated data for 50 incapable line-width profiles (Pakzad et al., 2024)

NO.	y_1	NO.	y_1	NO.	y_2	NO.	y_2	NO.	y_3	NO.	y_3
14	0.979558	39	1.12146	14	3.59186	39	3.504251	14	8.903957	39	9.044768
15	1.05656	40	0.81636	15	3.635777	40	3.367481	15	9.105234	40	8.980492
16	0.965508	41	0.975678	16	3.491407	41	3.369253	16	9.022381	41	9.012366
17	0.97351	42	0.961897	17	3.335233	42	3.493283	17	9.152333	42	8.984162
18	1.13328	43	1.017401	18	3.409412	43	3.554403	18	8.815971	43	8.836829
19	1.125294	44	1.016773	19	3.377803	44	3.738864	19	8.990528	44	8.981821
20	1.126102	45	0.900177	20	3.715595	45	3.416878	20	8.890523	45	8.927795
21	1.052278	46	0.982825	21	3.421955	46	3.501446	21	9.297993	46	8.913159
22	0.866259	47	0.969477	22	3.55696	47	3.474733	22	9.091797	47	8.895616
23	1.056807	48	1.047943	23	3.463851	48	3.291531	23	9.146618	48	8.957278
24	1.147193	49	1.094033	24	3.570872	49	3.439442	24	8.90534	49	8.811839
25	1.0342	50	1.095618	25	3.40718	50	3.305227	25	8.963707	50	9.105559

Table X. Simulated data for 50 capable line-width profiles (Pakzad et al., 2024)

NO.	y_1	NO.	y_1	NO.	y_2	NO.	y_2	NO.	y_3	NO.	y_3
1	1.0180593	26	1.0138177	1	3.4942656	26	3.4553197	1	8.9645595	26	8.9515202
2	0.9845577	27	0.9777184	2	3.4190235	27	3.473227	2	9.0081886	27	8.9281095
3	0.9836431	28	0.9971942	3	3.5417802	28	3.5000245	3	9.0245125	28	9.067467
4	0.9362899	29	0.9562642	4	3.5019471	29	3.4667	4	9.0365488	29	9.0101031
5	1.048989	30	1.0392712	5	3.4912849	30	3.5104055	5	8.9869747	30	9.0066934
6	0.9775365	31	0.9013341	6	3.5148607	31	3.5072092	6	8.9954327	31	9.0666172
7	0.9414777	32	1.0140255	7	3.499115	32	3.4053204	7	9.1356295	32	9.046982
8	1.0696265	33	0.9331546	8	3.4244996	33	3.424098	8	8.8700143	33	9.031823
9	0.9718575	34	0.965027	9	3.4728302	34	3.4369292	9	9.1483925	34	9.0876531
10	0.9492625	35	1.0200892	10	3.4738402	35	3.4514001	10	9.0310391	35	9.0677748
11	0.9675785	36	1.0502548	11	3.4498993	36	3.4630147	11	9.0721338	36	9.0249725
12	0.9332031	37	0.9164729	12	3.5872409	37	3.4836735	12	8.9068719	37	8.9672769
13	0.9163184	38	1.0639987	13	3.4285785	38	3.2950001	13	8.9735002	38	8.9696841
14	1.1424878	39	1.0267487	14	3.452889	39	3.4545514	14	8.9928517	39	9.0840461
15	1.0884905	40	0.9815903	15	3.4387344	40	3.5599691	15	9.0363211	40	8.9101182
16	1.0048764	41	0.9736904	16	3.4100636	41	3.4167325	16	8.9064975	41	9.0085826
17	0.9078209	42	0.9723019	17	3.4709754	42	3.5408192	17	9.0393555	42	8.889213
18	0.932115	43	0.9669982	18	3.4658994	43	3.5046304	18	8.9348671	43	9.0734015
19	0.9748496	44	0.9872295	19	3.5778104	44	3.4811008	19	9.0142058	44	9.0635523

Continue Table X. Simulated data for 50 capable line-width profiles (Pakzad et al., 2024)

NO.	y_1	NO.	y_1	NO.	y_2	NO.	y_2	NO.	y_3	NO.	y_3
20	1.0348915	45	0.9889815	20	3.467453	45	3.4942175	20	9.0505656	45	9.0101721
21	0.9031758	46	1.0370407	21	3.4168868	46	3.3858196	21	9.0303875	46	9.005706
22	0.8412783	47	1.0805184	22	3.5823625	47	3.477656	22	9.0772558	47	8.8558758
23	0.8959125	48	1.0147627	23	3.5594871	48	3.5823928	23	9.072507	48	9.0461501
24	1.0064877	49	0.9727915	24	3.4686563	49	3.4890005	24	8.9697242	49	8.8741033
25	1.0100757	50	1.0245806	25	3.3894729	50	3.4854664	25	9.0260452	50	8.866235

For the first data set with $\sigma = 0.099$ (incapable process), the values of MC_{pk} is estimated as 0.1238. Since the index MC_{pk} is less than one, the process is deemed incapable. For the second data set with $\sigma = 0.06203$ (capable process), The MC_{pk} index is equal to 1.2362, for the profile with $\sigma = 0.06203$, which indicates a capable process.

It should be noted that these obtained results agree with those reported by (Pakzad et al., 2024). However, the proposed method has the ability to represent SLP capability by one number jointly instead of calculating two separate indices $C_{pm_{b_0}}$ and $C_{pm_{b_1}}$.

B. Example 2

To demonstrate the practical application of our proposed method, we analyzed a real-world dataset from the leather industry, as presented by (Amiri, 2011). Leather quality is crucial in shoe production, and the dyeing process significantly impacts this quality. When shoe temperatures rise, sweat can cause the dye to stain socks. Therefore, evaluating the performance of the leather dyeing process is essential. The relationship between color effluent and temperature can be modeled in this process as the SLP. The response variable is color effluent, and the explanatory variable is temperature, with five levels: 25, 32, 39, 46, and 53 degrees Celsius (°C). A set of historical data, presented in Table XI, shows that based on 11 in-control profile samples, the reference profile is $Y = -0.0505 + 0.0034\,X$, where $\varepsilon_{ij} \sim N(0,0.0005)$. The functional SLs for color effluent at each temperature level are defined as $LSL_Y(X) = -0.09 + 0.0035X$ and $USL_Y(X) = -0.01 + 0.0035X$, as described by (Karimi Ghartemani et al., 2016).

Table XI In-control leather industry dataset (Amiri, 2011)

Profile \ Temperature	25	32	39	46	53
1	0.02180	0.02878	0.09083	0.10111	0.12566
2	0.03020	0.05422	0.07183	0.11716	0.13127
3	0.02880	0.02868	0.08575	0.09310	0.13549
4	0.03060	0.07571	0.01011	0.11624	0.12850
5	0.04880	0.02806	0.08549	0.11812	0.11880
6	0.03100	0.09438	0.07157	0.11922	0.14965
7	0.02310	0.07626	0.08093	0.13988	0.15714
8	0.04550	0.09253	0.15109	0.08746	0.14101
9	0.02090	0.04746	0.10231	0.12651	0.12299
10	0.05780	0.05227	0.11557	0.11261	0.11202
11	0.04630	0.06435	0.08679	0.07877	0.10632

To apply the proposed method in section III, we obtained a transformed model as $Y = 0.0821 - 0.0034\,X'$ with profile SLs as $USL_i = 0.1265 + 0.0035X_i'$ and $LSL_i = 0.0465 + 0.0035X_i'$. Then, based on Equations (12) and (13), the SLs of intercept and slope parameters are obtained as $-0{,}0005 \leq b_0 \leq 0{,}1735$ and $0{,}0027 \leq b_1 \leq 0{,}0043$, respectively. Then, based on Equations (4) and (7), the $p_{b_0} = 1$, and $p_{b_1} = 0.5943$ are obtained indicated. Finally, the value of MC_{pk} is estimated as 0.0795. Thus, as the index MC_{pk} is less than one, we state that the SLP is not capable. The estimated values of the $C_{pm_{b_0}}$and $C_{pm_{b_1}}$were also obtained as 2.6665 and 0.2772, respectively. Given that the process is deemed incapable due to incapability in the slope parameter, this finding aligns with the proposed method's prediction of a higher nonconformity rate for slope compared to intercept.

VI. CONCLUSION

In this paper, the composite capability index, MC_{pk}, for SLP parameters was introduced. A comprehensive simulation study was conducted to evaluate the performance of the proposed and existing indices in terms of accuracy and precision. The simulation results demonstrated the superior performance of the proposed index estimation compared to existing methods across all simulated scenarios. This is confirmed by smaller MAE and MSE values, which indicate have closer values to their true values. The superiority of the proposed index is particularly pronounced in scenarios with limited data, making it a valuable tool for practical applications. Two real-world case studies were provided to demonstrate the proposed index's applicability. Future research will focus on the extension of the proposed index for more complex profiles, such as multivariate, polynomial, non-linear profiles, as well as in multi-stage processes with profile quality characteristics.

REFERENCES

Abbasi, S. A., Abbas, T., & Adegoke, N. A. (2021). Improved simple linear profiling method with application to chemical gas sensors. *Quality and Reliability Engineering International*, *37*(8), 3179-3191.

Adibfar, S., & Noorossana, R. (2022). Process Capability Analysis for Simple Linear Profiles in Two-stage Process. *Journal of Industrial Engineering Research in Production Systems*, *10*(20), 183-191.

Adibfar, S., & Noorossana, R. (2024). Process Capability Analysis for Simple Linear Profiles in Multistage Processes. *Pakistan Journal of Statistics and Operation Research*, 139-155.

Alevizakos, V., Koukouvinos, C., & Castagliola, P. (2019). Process capability index for Poisson regression profile based on the S pmk index. *Quality Engineering*, *31*(3), 430-438.

Amiri, A. (2011, January). Monitoring Simple Linear Profiles in the Leather Industry-A Case Study. In *2011 the 2nd International Conference on Industrial Engineering and Operations Management*. 2011 the 2nd International Conference on Industrial Engineering and Operations Management.

Bothe, D. R. (1997). *Measuring process capability: techniques and calculations for quality and manufacturing engineers*. McGraw-Hill Companies.Bothe, D. R. (1999). Composite capability index for multiple product characteristics. *Quality Engineering*, *12*(2), 253-258.

Boyles, R. A. (1991). The Taguchi capability index. *Journal of quality technology*, *23*(1), 17-26.

Chiang, J. Y., Lio, Y. L., & Tsai, T. R. (2017). MEWMA control chart and process capability indices for simple linear profiles with within-profile autocorrelation. *Quality and Reliability Engineering International*, *33*(5), 1083-1094.

de-Felipe, D., & Benedito, E. (2017). A review of univariate and multivariate process capability indices. *The International Journal of Advanced Manufacturing Technology*, *92*, 1687-1705.

Derakhshani, R., Esmaeeli, H., & Amiri, A. (2021). Monitoring binary response profiles in multistage processes. *Journal of Quality Engineering and Production Optimization*, *6*(2), 97-114.

Ebadi, M., & Shahriari, H. (2013). A process capability index for simple linear profile. *The International Journal of Advanced Manufacturing Technology*, *64*, 857-865.

FakhimiKazemi, H., Ahmadi, O., & Izadbakhsh, H. (2023). Monitoring of simple linear profiles and change point estimation in the presence. *Journal of Quality Engineering and Production Optimization*, *8*(1).

Ganji, Z. A., & Gildeh, B. S. (2023). A new process capability index for simple linear profile. *Communications in Statistics-Theory and Methods*, *52*(11), 3879-3894.

Guevara G, R. D., & Alejandra Lopez, T. (2022). Process capability vector for multivariate nonlinear profiles. *Journal of Statistical Computation and Simulation*, *92*(6), 1292-1321.

Guevara, R. D., & Vargas, J. A. (2016). Evaluation of process capability in multivariate nonlinear profiles. *Journal of Statistical Computation and Simulation*, *86*(12), 2411-2428.

Guevara, R. D., & Vargas, J. A. (2015). Process capability analysis for nonlinear profiles using depth functions. *Quality and Reliability Engineering International*, *31*(3), 465-487.

Hosseinifard, S. Z., & Abbasi, B. (2012a). Evaluation of process capability indices of linear profiles. *International Journal of Quality & Reliability Management*, *29*(2), 162-176.

Hosseinifard, S. Z., & Abbasi, B. (2012b). Process capability analysis in non normal linear regression profiles. *Communications in Statistics-Simulation and Computation*, *41*(10), 1761-1784.

Kane, V. E. (1986). Process capability indices. *Journal of quality technology*, *18*(1), 41-52..

Kang, L., & Albin, S. L. (2000). On-line monitoring when the process yields a linear profile. *Journal of quality Technology*, *32*(4), 418-426.

Karimi Ghartemani, M., Noorossana, R., & Niaki, S. T. A. (2016). A new approach in capability analysis of processes monitored by a simple linear regression profile. *Quality and Reliability Engineering International*, *32*(1), 209-221.

Kim, K., Mahmoud, M. A., & Woodall, W. H. (2003). On the monitoring of linear profiles. *Journal of Quality Technology*, *35*(3), 317-328.

Kutner, Michael .. .., Christopher. J. Nachtsheim, John Neter, and William Li. 1996. *Applied Linear Regression Models*. Fifth. McGraw-Hill, Boston.

Mahmoud, M. A., & Woodall, W. H. (2004). Phase I analysis of linear profiles with calibration applications. Technometrics, 46(4), 380-391.

Maleki, M. R., Amiri, A., & Castagliola, P. (2018). An overview on recent profile monitoring papers (2008–2018) based on conceptual classification scheme. *Computers & Industrial Engineering*, *126*, 705-728.Natrella, M. (2010). *NIST/SEMATECH e-handbook of statistical methods. Nist/Sematech*, *49*.

Nemati Keshteli, R., Baradaran Kazemzadeh, R., Amiri, A., & Noorossana, R. (2014). Developing functional process capability indices for simple linear pro le. *Scientia Iranica*, *21*(3), 1096-1104.

Nemati Keshteli, R., Kazemzadeh, R. B., Amiri, A., & Noorossana, R. (2014). Functional process capability indices for circular profile. *Quality and Reliability Engineering International*, *30*(5), 633-644.

Saghaei, A., & Noorossana, R. (2011). Introduction to profile monitoring. *Statistical Analysis of Profile Monitoring*, 1-20. doi: 10.1002/9781118071984.ch1

Pakzad, A., Adibfar, S., Razavi, H., & Noorossana, R. (2024). Process capability analysis for simple linear profiles. *Quality & Quantity*, *58*(3), 2183-2211.

Pakzad, A., & Basiri, E. (2023). A new incapability index for simple linear profile with asymmetric tolerances. *Quality Engineering*, *35*(2), 324-340.

Pakzad, A., Razavi, H., & Sadeghpour Gildeh, B. (2022). Developing loss-based functional process capability indices for simple linear profile. *Journal of Statistical Computation and Simulation*, *92*(1), 115-144.

Pakzad, A., Razavi, H., & Sadeghpour Gildeh, B. (2021). Functional process capability indices for a simple linear profile in fuzzy environment. *Journal of Industrial and Systems Engineering*, *13*(4), 1-22.

Pour Larimi, A. M., Nemati Keshteli, R., & Safaei, A. S. (2019). Functional process capability indices for nonlinear profile. *Journal of Industrial and Systems Engineering*, *12*, 1-14.

Amiri, A., & Rezaye Abbasi Charkhi, M. (2015). Process capability index for logistic regression profile based on SPMK index. *International Journal of Engineering*, *28*(8), 1186-1192.

Rezaye Abbasi Charkhi, M., Aminnayeri, M., & Amiri, A. (2016). Process capability indices for logistic regression profile. *Quality and Reliability Engineering International*, *32*(5), 1655-1661.

Shahriari, H., & Sarrafian, M. (2009). Assessment of process capability in linear profiles. In *Proceedings of the 6th international industrial engineering conference, Tehran, Iran (in Farsi)*.

Sogandi, F., & Amiri, A. (2023). A Robust Control Chart for Monitoring Autocorrelated Multiple Linear Profiles in Phase I. *International Journal of Engineering*, *36*(8), 1429-1439.

Wang, F. K. (2014). A process yield for simple linear profiles. *Quality Engineering*, *26*(3), 311-318.

Wang, F. K. (2015). Measuring the process yield for circular profiles. *Quality and Reliability Engineering International*, *31*(4), 579-588.

Wang, F. K. (2016). Process yield analysis for multivariate linear profiles. *Quality Technology & Quantitative Management*, *13*(2), 124-138.

Wang, F. K., & Guo, Y. C. (2014). Measuring process yield for nonlinear profiles. *Quality and Reliability Engineering International*, *30*(8), 1333-1339.

Wang, F. K., & Tamirat, Y. (2014). Process yield analysis for autocorrelation between linear profiles. *Computers & Industrial Engineering*, *71*, 50-56.Wang, F. K., & Tamirat, Y. (2015). Process yield analysis for linear within-profile autocorrelation. *Quality and Reliability Engineering International*, *31*(6), 1053-1061.

Woodall, W. H., Spitzner, D. J., Montgomery, D. C., & Gupta, S. (2004). Using control charts to monitor process and product quality profiles. *Journal of Quality Technology*, *36*(3), 309-320. doi:10.1080/00224065.2004.11980276

Wu, X. F. (2016). An assessment approach for process capability in simple linear profile. *In Proceedings of the 22nd International Conference on Industrial Engineering and Engineering Management 2015: Core Theory and Applications of Industrial Engineering (Volume 1)* (pp. 613-620). Atlantis Press.

Yeganeh, A., Abbasi, S. A., Shongwe, S. C., Malela-Majika, J. C., & Shadman, A. R. (2024). Evolutionary support vector regression for monitoring Poisson profiles. *Soft Computing*, *28*(6), 4873-4897.

Yeganeh, A., & Shadman, A. (2021). Monitoring linear profiles using Artificial Neural Networks with run rules. *Expert Systems with Applications*, *168*, 114237.